A Statistical Study of Beam Centroid Oscillations in a Solenoid Transport Channel

S. Lund, C. Wootton, J. Coleman, S. Lidia, P. Seidl

May 11, 2009

Disclaimer

This document was prepared as an account of work sponsored by an agency of the United States government. Neither the United States government nor Lawrence Livermore National Security, LLC, nor any of their employees makes any warranty, expressed or implied, or assumes any legal liability or responsibility for the accuracy, completeness, or usefulness of any information, apparatus, product, or process disclosed, or represents that its use would not infringe privately owned rights. Reference herein to any specific commercial product, process, or service by trade name, trademark, manufacturer, or otherwise does not necessarily constitute or imply its endorsement, recommendation, or favoring by the United States government or Lawrence Livermore National Security, LLC. The views and opinions of authors expressed herein do not necessarily state or reflect those of the United States government or Lawrence Livermore National Security, LLC, and shall not be used for advertising or product endorsement purposes.

A STATISTICAL STUDY OF BEAM CENTROID OSCILLATIONS IN A SOLENOID TRANSPORT CHANNEL [*]

Steven M. Lund,

Lawrence Livermore National Laboratory, Livermore, CA 94550

Christopher J. Wootton, Joshusa E. Coleman, Steve M. Lidia, and Peter A. Seidl

Lawrence Berkeley National Laboratory, Berkeley, CA 94720

Abstract

A recent theory of transverse centroid oscillations in solenoidally focused beam transport lattices presented in Ref. [1] is applied to statistically analyze properties of the centroid orbit in the Neutralized Drift Compression Experiment (NDCX) at the Lawrence Berkeley National Laboratory. Contributions to the amplitude of the centroid oscillations from mechanical misalignments and initial centroid errors exiting the injector are analyzed. Measured values of the centroid appear consistent with expected alignment tolerances. Correction of these errors is discussed.

INTRODUCTION

In solenoid transport control of the beam centroid (center of mass) can be challenging. A linear (small-amplitude) centroid orbit can be decomposed into two parts: an overall angular "Larmor" rotation phase proportional to the axial field[1, 2], and superimposed x-y plane decoupled transverse beatron oscillations within the rotating frame. Mechanical misalignments of the solenoids result in dipole bending terms that drive an aligned beam centroid off-axis. These combined effects can result in centroid orbit oscillations with intricate structure. The x-y coupling in the laboratory frame also complicates correction of the centroid orbit with steering dipoles.

Reference [1] presents a framework to efficiently analyze small-amplitude (linear) oscillations of the transverse beam centroid in solenoidal transport channels. This theory employs a transformation to a rotating Larmor frame to simply express the contributions to the centroid response from mechanical misalignments (transverse center displacements and tilts/rotations about the of the longitudinal axis of symmetry) of the solenoid and initial values (errors) of the centroid in phase-space. The centroid evolution is expressed in terms of a superposition of the centroid evolving in the ideal aligned system from an specified initial condition plus an expansion in terms of "alignment functions" that are functions of only the ideal lattice with corresponding amplitudes set by the solenoid misalignment parameters. Applications of this formulation were developed for efficient statistical analysis of centroid deviations, calculation of actual lattice misalignments from centroid measurements, and optimal beam steering.

We apply the formulation in Ref. [1] here to analyze statistical properties of beam centroid oscillations in the NDCX experiment[3]. It is shown that both mechanical center displacements and tilt misalignments of the solenoids are important. Larger than first anticipated centroid errors are shown to be consistent with expected ranges of misalignment parameters. This suggests that efficient centroid steering corrections will be a necessary part of similar future experiments.

THE NDCX SOLENOID LATTICE

The NDCX solenoid lattice is illustrated in Fig. 1. A planar, K^+ source is located at (reference) axial coordinate $z = 0$. The source is pulsed such that a 5–10 μs, 300 keV beam emerges from the extraction electrode aperture at $z = 0.12$ m. This injected beam has radius $r_b = 1$ cm, flat-top current $I \sim 26$ mA, and rms edge-emittance $\varepsilon \sim 14$ mm-mrad. Four identical solenoids are arranged in a lattice with period $L_p = 0.6$ m. The axial center of the first solenoid is at $z = 0.462$ m. Three identical cross-field steering dipoles are inserted between solenoids as indicated with the axial center of the first dipole element at $z = 0.764$ m. Diagnostic measurements of the transverse beam phase-space are made at $z = 2.62$ m (measurements of full position, angle phase-space: x, x', and y, y') and $z = 2.68$ m (x, and y only) using a scintillator-based optical beam imager. Here, we denote $\langle x \rangle_\perp = x$ etc., where $\langle \cdots \rangle_\perp$ is an average over the transverse distribution. The beam centroid is measured over the pulse flat-top where little fluctuations are observed in low-order moments. Centroid coordinate measurements of x and y can be taken in a *single* shot with characteristic ± 0.1 mm resolution. Centroid angle measurements of x' and y' are based on series of images of a slit moved at stepped intervals over multiple shots and have characteristic ± 2 mrad resolution. Shot-to-shot repeatability of the machine is high.
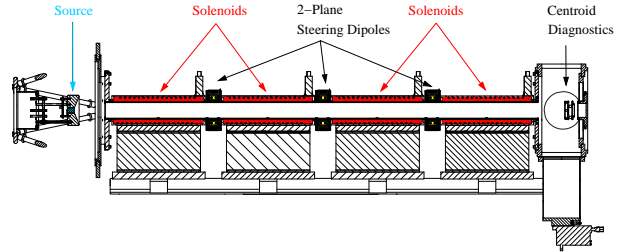

Figure 1: (Color) NDCX lattice with source, solenoids, cross-field steering dipoles, and the diagnostic measurement location indicated.

Solenoids in the NDCX are adequately modeled in terms of their on-axis field strength $B_{z0}(z) = B_z(\mathbf{x}_\perp = 0)$ as:

$$\mathbf{B}_\perp = -\frac{1}{2}\frac{\partial B_{z0}(z)}{\partial z}\mathbf{x}_\perp, \qquad B_z = B_{z0}(z)$$

Here, subscript $\perp$ denotes transverse components. In terms of a thin-sheet current model B_{z0} can be analytically calculated as[4] $B_{z0} = B_{\max}F(z)$ where $B_{\max}$ is the peak field strength and $F(z) = f(z)/f(z=0)$ with

$$f(z) = \frac{1}{2}\left(\frac{\ell/2 - z}{\sqrt{(\ell/2-z)^2 + R^2}} + \frac{\ell/2 + z}{\sqrt{(\ell/2+z)^2 + R^2}}\right)$$

is a fringe function. Here, R and ℓ are the radius and length of the thin current sheet coil. The actual magnet coils are four layer with an axial length of 433.1 mm and inner and outer radii of 50.8 mm and 66.0 mm. On-axis field measurements of $B_{z0}(z) = B_z(\mathbf{x}_\perp = 0, z)$ were made at approximately 80 steps in z for the four magnets, first in one orientation and then with the ends flipped. A nonlinear regression fit to $F(z) = B_{z0}(z)/B_{z0}(0)$ obtained best fit parameters of $\ell = 436.9$ mm and $R = 60.3$ mm. This fit is plotted superimposed with the data sets in Fig. 2. The data has excellent agreement with the fringe model in both the central and far fringe regions. Coil currents are maximum, and essentially constant over the beam pulse and are set to within 1% of target values. Maximum solenoid coil excitations produce a peak field of $B_{\max} \sim 3$ Tesla. Calibration data relating the coil current to the peak field has been consistently obtained from detailed 3D magnet simulations, experimental field measurements, and comparisons of measured beam envelope to simulations.
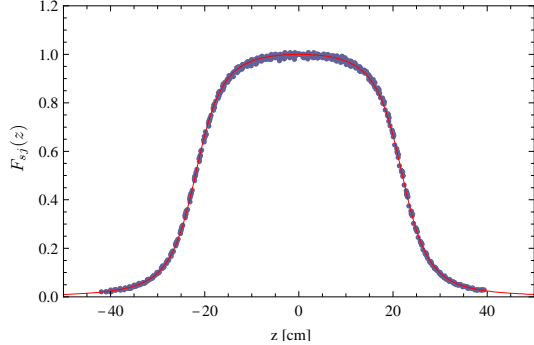
Figure 2: (Color) Best fit of the thin coil model (red curve) to measured solenoid data (blue dots).

The solenoids are placed in the lattice using linear superposition. A typical NDCX operating point with solenoid strengths $B_{\max} = 2.60, 1.00, 0.80$ and 2.05 Tesla is taken. These values are consistent matching the full beam envelope with a subsequent lattice that focuses, neutralizes, and drift compresses the beam. The axial magnetic field B_z and the transverse field gradient $\partial B_r/\partial r = \nabla_\perp \cdot \mathbf{B}_\perp/2$ of the superimposed solenoids are plotted in Fig. 3(a) and (b). The Larmor frame rotation angle $\tilde{\psi}$ shown in Fig. 3(c) is proportional to the integral of B_{z0}^2 times kinematic factors and represents the macroscopic rotation angle of the beam[1, 2]. Note that the rate of change of $\tilde{\psi}$ changes as the beam enters and exits solenoid fringe fields. Axial extents of the solenoid coils are indicated in red in Figs. 3 and in subsequent figures.
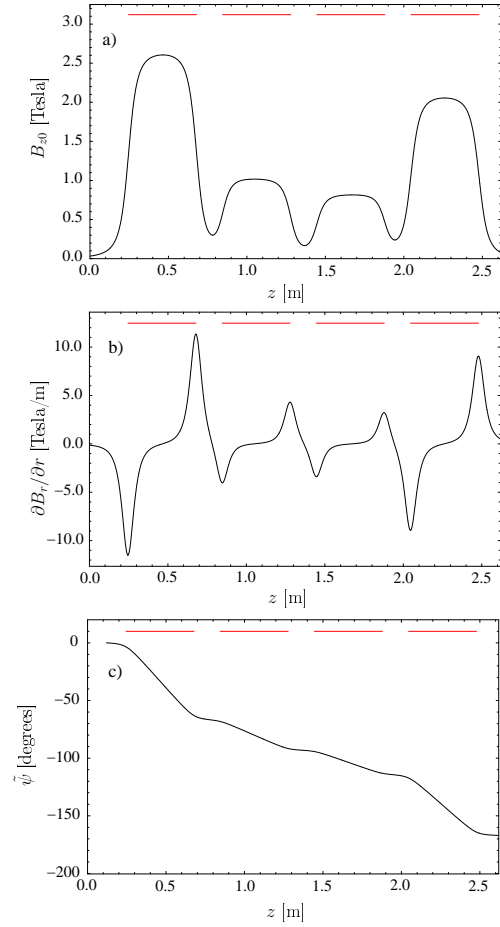
Figure 3: (Color) Axial magnetic field B_{z0} (a), transverse magnetic field gradient $\partial B_r/\partial r$ (b), and Larmor frame rotation angle $\tilde{\psi}$ (c) versus axial coordinate s.

STATISTICAL ANALYSIS
OF CENTROID EXCURSIONS

Analysis of the centroid orbits shows [1] that for small-amplitude excursions, mechanical misalignments of the solenoids can be described in terms of transverse displacements of the geometric center (Δ_x and Δ_y) and angular rotations (tilts) of the ideal axis of symmetry of the magnet (Θ_x and Θ_y). The longitudinal center shift Δ_z is not important to leading order and only two tilt angles are necessary because the ideal solenoid is rotationally symmetric about its axis of symmetry. Although the mechanical placements of the magnets are accurate, deformations in coil windings can give effective misalignment parameters with $|\Delta_{x,y}| <\sim 1.5$ mm and $|\Theta_{x,y}| <\sim 5$ mrad. The initial centroid emerging from the injector can also be misaligned due to mechanical alignment and beam nonuniformities. Initial centroid errors are expected to be bounded as $|x|, |y| <\sim 2$ mm and $|x'|, |y'| <\sim 5$ mrad.

A uniform distribution of errors is assumed out to plus and minus the maximum amplitudes listed above and an ensemble of 100k independent errors was taken. Calculated rms x and x' centroid coordinates are shown in Fig. 4(a) and (b). Only the x and x' are shown since y and y' are identical for an infinite ensemble. rms contributions

to the orbit from only centroid initial conditions (x_i, y_i, x'_i, y'_i), only solenoid displacements ($\Delta_{x,y}$), only solenoid rotations ($\Theta_{x,y}$), and then all error sources combined are shown. The contributions to the mean square statistical values add in quadrature. Note that the contribution due to rotations is largest. The initial condition contribution at first dominates those due to solenoid misalignment but by the end of the first solenoid misalignments induced by dipole kicks from the displacement and rotational misalignments become larger than the amplitude initial condition contribution. Contrasting Figs. 3 and 4, note that increasing field strength leads to larger centroid excursions – both for solenoid misalignment contributions and initial condition contributions. The former results simply from the misalignment induced dipole kicks becoming larger with increasing field strength. The latter can be understood in terms of maximum excursion projections of Courant-Snyder invariants of centroid orbit in the absence of errors becoming larger where focusing is stronger.
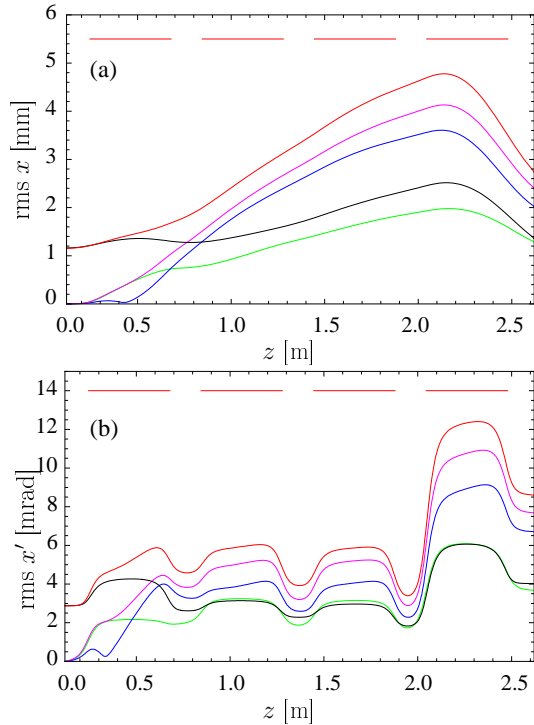
Figure 4: (Color) rms centroid coordinate x (a) and angle x' (b) for an ensemble of errors and $B_{max} = 2.6$, 1.4, 1.06, and 2.35 Tesla. Key: Red (All), Magenta ($\Delta_{x,y}$ and $\Theta_{x,y}$), Blue ($\Theta_{x,y}$), Green ($\Delta_{x,y}$), Black (initial x, x', y, y')

Measured centroid data (see Table 1) at the end of the NDCX lattice appear reasonably consistent with the statistical analysis of the centroid errors. Keep in mind that the orbit for a particular sample set of errors can vary significantly from the one rms values presented. x-orbits for 75 sample sets of errors are shown in Fig. 5 together with the $\pm$ rms values of the ensemble. The formulation can also be exploited to efficiently calculate maximum (worst case) excursions within the ensemble which are much larger than the probable rms values.

Table 1: Centroid phase-space measured before (Nom) and after steering (Steered).

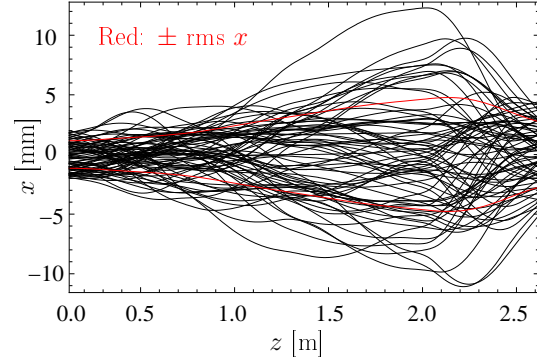| Case	x [mm]	x' [mrad]	y [mm]	y' [mrad]
Nom	-5.81	2.24	-2.77	3.37
Steered	-0.15	0.51	0.00	-0.31

Figure 5: (Color) x-orbits for 75 error sets and the corresponding $\pm$ rms values in Fig. 4.

DISCUSSION

The significant expected values of centroid excursions measured at the end of the NDCX necessitate the use of steering dipoles within the lattice in order to maintain precise control of the beam on target and to limit deleterious processes that scale with centroid amplitude (image fields, nonlinear focusing, energy-spread induced centroid corkscrew, etc.). At first the centroid excursions after the four solenoids were thought to be anomalously large given the precision of the mechanical alignment of the magnet frames. Later this was understood to result from effective degradations of the alignment parameters due to manufacturing steps in the coils (rigid conductor wound) which can not be easily controlled. An experimental procedure based on accumulating a deviation Jacobian was used to steer the beam centroid back on axis to measurement precision (see Table 1). Although successful, this procedure is labor intensive and must be repeated whenever the strengths of the solenoids and/or beam energy change. Ongoing work is applying the formulation of Ref. [1] to calculate actual lattice alignment errors and thereby enable lattice correction or optimal beam steering.

ACKNOWLEDGMENTS

REFERENCES

[1] S.M. Lund, C.J. Wootton, and E.P. Lee, *Transverse centroid oscillations in solenoidally focused beam transport lattices*, in press, Nuc. Inst. Meth. A. (2009).

[2] H. Wiedemann, *Particle Accel. Physics II*, Springer, 1995.

[3] P.A. Seidl et. al, *Progress in beam focusing and compression for WDM experiments*, in press, Nuc. Inst. Meth. A. (2009).

[4] E.P. Lee and M. Leitner, *Solenoid Fields for Ion Beam Transport and Focusing*, Report LBNL-6317, LBNL (2007).